Blast Wave Calculations in Argon Cavity Gas for Light Ion Beam Fusion Reactors

R.R. Peterson and G.A. Moses

October 1979

UWFDM-315

FUSION TECHNOLOGY INSTITUTE

UNIVERSITY OF WISCONSIN

MADISON WISCONSIN

Blast Wave Calculations in Argon Cavity Gas for Light Ion Beam Fusion Reactors

R.R. Peterson and G.A. Moses

Fusion Technology Institute
University of Wisconsin
1500 Engineering Drive
Madison, WI 53706

http://fti.neep.wisc.edu

October 1979

UWFDM-315

BLAST WAVE CALCULATIONS IN ARGON CAVITY GAS FOR LIGHT ION BEAM FUSION REACTORS

R. R. Peterson

G. A. Moses

October 1979

Fusion Engineering Program
Nuclear Engineering Department
University of Wisconsin
Madison WI 53706

UWFDM-315

Abstract

Blast wave calculations are performed for a 30 MJ explosion in a 4 meter light ion beam reactor cavity containing 50 torr of Argon gas using a hydrodynamic-radiative transfer computer code. These results are compared to strong shock theory. The heat flux and overpressure at the first wall arecomputed for different initial cavity gas temperatures. The effects of changing the cavity gas type to a diatomic rather than monatomic molecule are also considered.

I. Introduction

A major problem in the design of inertial confinement fusion reactors is the potential for damage to the reactor first wall due to X-rays and charged particle debris from the exploding fusion pellet. Escaping 14.1 MeV neutrons account for 70-80% of the fusion energy while the remaining 20-30% is in the form of X-rays and pellet debris. The neutrons have long mean free paths and hence volumetrically heat the reactor blanket and first wall. The X-rays and charged particle debris have short mean free paths in solids, so they represent a surface heat load on the first wall. This can result in unacceptably high surface temperature rises and thermal stresses.

In the case of light ion beam reactor designs the cavity is filled with a gas that serves as the transport medium for propagation of the ion beams from the diodes to the target. This gas is also dense enough to stop the target X-rays and debris in a small volume surrounding the target.[1] This protects the first wall from direct bombardment by the exploding target but the X-ray and debris energy are instead transformed into a blast wave that propagates to the first wall. A blast wave is a fireball of hot plasma and radiant energy in equilibrium, trapped behind a propagating shock wave.[5] The shock wave is driven outward into the cold gas by the pressure of this fireball behind it. When it reaches the first wall it transfers a large mechanical impulse through a brief but high pressure pulse. Also, under the proper conditions, radiant energy may also be released from the fireball before the shock can reach the first wall. This release of thermal X-rays can cause sharp temperature rises and large thermal stresses in the first wall.

It is, therefore, very important to understand the dynamics of this fireball creation and propagation to the first wall if one is to design the first wall of a light ion beam fusion reactor. In the second part of this report, we describe a hydrodynamic-radiative transfer computer code, FIRE, that has been developed to model fireball behavior. In part III we review the strong shock theory treatment of blast waves of Taylor.[2-4] Results of our computer model are presented in part IV for Argon cavity gas. The conclusions of this study are presented in part V.

II. Model and Computational Method

In studying the development of fireballs, we have taken a one fluid-two temperature approximation for the gas-radiation system. The gas ions and electrons are assumed to be in local thermal equilibrium at a temperature T_p and to experience hydrodynamic transport as a single fluid. The radiation is assumed to have a blackbody spectrum at a local temperature T_r, independent from the gas temperature T_p. The transport of radiant energy is treated separately from the transport of the plasma energy by thermal conduction.

A fully implicit gas hydrodynamic radiative-transfer code, FIRE, has been used to implement this model. Using one-dimensional (planar, $\delta = 1$; cylindrical, $\delta = 2$; spherical, $\delta = 3$) Lagrangian coordinates, the spatial variable x may be replaced by the Lagrangian mass,

$$dm_o = x^{\delta-1} \rho(x)dx \ , \qquad (1)$$

where $\rho(x)$ is the mass density. In these coordinates, the one-fluid equation of motion is

$$\frac{du}{dt} = -x^{\delta-1} \frac{\partial}{\partial m_o} (P + Q) \ , \qquad (2)$$

where u is the fluid velocity, $P = P_{gas} + P_{radiation}$ and Q is the von-Neumann artificial viscosity.[6] The artificial viscosity insures that the total pressure P + Q is continuous across the shock and is written as

$$Q_{j-\frac{1}{2}} = \begin{cases} 2(\ell^3/V)\left(\frac{\partial u}{\partial x}\right)^2 & \text{under compression} \\ 0 & \text{under expansion,} \end{cases} \tag{3}$$

where ℓ is a constant with units of length and V is the specific volume. This common numerical recourse contributes additional heating to the gas at the shock front. The equation of motion is solved by using a standard explicit finite-difference method.[7] An important consideration in determining the time step Δt is that the shock must not traverse a fluid zone in a single time step, a stipulation which is known as the Courant condition[8] and is written

$$C_s \, \Delta t < \Delta x, \tag{4}$$

where C_s is the speed of sound (local) and Δx is the width of the zone.

Since the gas and the radiation field have separate temperatures, there are two energy equations describing this hydrodynamic system. Coupled by a radiation-gas equilibration term, these energy equations are

$$C_{vp} \frac{\partial T_p}{\partial t} = \frac{\partial}{\partial m_o}\left(x^{\delta-1} K_p \frac{\partial T_p}{\partial x}\right) - \omega_{pr}(T_p - T_r) - (P_p)_T \frac{\partial V}{\partial t} T_p \tag{5}$$

and

$$C_{vr} \frac{\partial}{\partial t} T_r = \frac{\partial}{\partial m_o}\left(x^{\delta-1} K_r \frac{\partial}{\partial x} T_r\right) + \omega_{pr}(T_p - T_r) - (P_r)_T \frac{\partial V}{\partial t} T_r \, . \tag{6}$$

K_p is the thermal conductivity of the gas, which we assume is due to electron collisions and is assumed to be of the classical (Spitzer) form[9] for a Lorentz gas. The compressional terms are proportional to the rate of change of the specific volumes, $\frac{\partial V}{\partial t}$, and contain $(P_p)_T \equiv \frac{\partial P_p}{\partial T_p}$ and $(P_r)_T \equiv \frac{\partial P_r}{\partial T_r}$. The power flow from the gas to the radiation is taken as proportional to

$$\omega_{pr} = \begin{cases} c\, C_{vr}/\ell_1 & ; \quad T_p \le T_r \\ c\, C_{vr}(T_p/T_r)^3/\ell_1 & ; \quad T_p > T_r \end{cases} , \tag{7}$$

where c is the speed of light. $K_r = 4\sigma\ell T_r^3$ is the radiation thermal conductivity where σ is the Stefan-Boltzmann constant. The radiation heat capacity $C_{vr} = 16\ T_r^3/c$ and the radiation pressure $P_r = 4\ T_r^4/3c$ are the classical blackbody values. The gas pressure $P_p = (1 + Z)T_pN_p$ assumes a perfect gas of Z free electrons per ion. The heat capacity of the gas is $C_{vp} = \partial E_p/\partial T_p$. The Planck mean free path ℓ_1, the Rosseland mean free path ℓ, the ionization state Z and the internal energy of the gas E_p are obtained from tables generated by the atomic and optical data code, MFP.[10] In MFP, the major mode of recombination has been assumed to be three body recombination so that the ionization is calculated within the Saha model[11] and the photons have been assumed to occur in a Planck spectrum.

To improve the numerical stability of the FIRE code, upstream averaging and flux limiting of radiant energy flux have been implemented. At the edge of the fireball, the radiant energy flux is so large that the amount of energy transported into a fluid zone in a time step may be as large as the radiant energy resident in the zone prior to the time step. Upstream averaging avoids a numerical instability caused by this large energy flux, by using the radiation temperature in the zone from whence comes the majority of the radiant energy to calculate the radiant transport parameters. Flux limiting insures that, even if the Rosseland mean free path is infinite, the radiant energy flux out of any zone is no larger than the speed of light times the radiant energy density in that zone. The flux limiting is brought into play in a smooth manner so that numerical stability is maintained.

For calculations presented in this paper, 50 spatial fluid zones are used along with 8,000 to 12,000 time steps. Equal mass zoning is used as much as possible to minimize artificially induced reflections of lighter zones off of heavy ones, with the most care being taken near the center and the wall.

III. Strong Shock Theory

The theories of Taylor and Sedov[2-4] are known to provide good approximations to the emanation of spherical blast waves from point explosions. These theories are only valid when a large amount of energy is held in the small volume behind in the wave. For this reason, the strong shock theory deviates from our numerical method when the distance traveled by the shock becomes large enough to significantly lower the energy density behind the shock. That the strong shock theory breaks down will be shown in Section IV.

The energy of the explosion E and the original mass density of the gas ρ_1 are the only parameters which influence the propagation of a strong shock. Thus, the only dimensionless combination of parameters and independent variables is

$$\xi_0 = r(\rho_1/E)^{\frac{1}{5}} t^{-\frac{2}{5}} \quad . \tag{8}$$

By requiring that ξ_0 is the same at any instant, we arrive at Taylor's famous formula,

$$r = \xi_0 (E/\rho_1)^{\frac{1}{5}} t^{\frac{2}{5}} . \tag{9}$$

If we assume that gas to be ideal, we may use the well established[12] ideal gas strong shock relations to obtain the velocity

$$v_2 = \frac{4r}{5t}\frac{1}{(\gamma + 1)}, \tag{10}$$

the density

$$\rho_2 = \frac{\rho_1(\gamma + 1)}{(\gamma - 1)}, \tag{11}$$

and the pressure

$$P_2 = \frac{8\rho_1 r^2}{25t^2}\frac{1}{(\gamma + 1)} \tag{12}$$

of the gas behind the shock. Here the subscript 1 pertains to quantities measured in front of the shock and the subscript 2 to those measured behind the shock. Using Eqs. (9)-(12) and conservation of mass and energy, we find that ξ_0 is only dependent upon the ratio of specific heats γ:[2]

$$\xi_0 = (\frac{5}{2})^{\frac{2}{5}}(\frac{3}{4\pi})^{\frac{1}{5}}(\frac{\gamma + 1}{2})^{\frac{2}{5}} \tag{13}$$

By combining Eqs. (9) and (12) we find that the pressure behind the shock wave is proportional to the energy density behind the shock:

$$P_2 = (\frac{2}{5})^2 \frac{2}{\gamma + 1}\ \xi_0{}^5 E/r^3 \tag{14}$$

The maximum pressure seen at the first wall is not P_2 but is P_3, the pressure behind a shock which has been reflected off the wall and is propagating into the gas, which is now at pressure P_2. The ratios of the three specific volumes in a perfect gas obey[12]

$$\frac{V_2}{V_1} = \frac{(\gamma + 1)P_1 + (\gamma - 1)P_2}{(\gamma - 1)P_1 + (\gamma + 1)P_2} \tag{15}$$

and

$$\frac{V_3}{V_1} = \frac{(\gamma + 1)P_2 + (\gamma - 1)P_3}{(\gamma - 1)P_2 + (\gamma + 1)P_3} \quad . \tag{16}$$

The relative velocity between the two sides of the shock is the same for the reflected wave as it is for the incident wave,[13] so that, because

$$v_1 - v_2 = \sqrt{(P_2 - P_1)(V_1 - V_2)} \tag{17}$$

we find

$$(P_2 - P_1)(V_1 - V_2) = (P_3 - P_2)(V_2 - V_3). \tag{18}$$

The specific volumes may be eliminated to yield

$$\frac{(P_2 - P_1)^2}{(\gamma + 1)P_1 + (\gamma - 1)P_2} = \frac{(P_3 - P_2)^2}{(\gamma - 1)P_2 + (\gamma + 1)P_3} \quad . \tag{19}$$

Besides the trivial solutions $P_3 = P_1$, we find that

$$P_3 = P_2\left(\frac{(3\gamma - 1)P_2 - (\gamma - 1)P_1}{(\gamma - 1)P_2 - (\gamma + 1)P_1}\right). \tag{20}$$

For $\gamma > 1$, the strong shock maximum pressure is

$$P_3 = P_2\left(\frac{3\gamma - 1}{\gamma - 1}\right). \tag{21}$$

IV. Results

A series of calculations have been done using the FIRE computer code to determine the overpressure and heat flux generated at the first wall of a light ion beam fusion reactor as the result of a 30 MJ explosion in a cavity filled with Argon gas. The important input parameters for these calculations are given in Table 1. It is assumed that 30 MJ of energy is instantaneously deposited in a 10 cm radius sphere surrounding the target. This 30 MJ yield implies a total yield of about 100 MJ when the 14.1 MeV neutrons are included. This energy deposition raises the temperature of the sphere of Argon gas to 64 eV. The mass of the target is assumed to be uniformly spread over this 10 cm sphere and for simplicity is assumed to have the same characteristics as Argon. This is taken to be the initial condition for the blast wave calculation. Five calculations have been done for differing initial temperatures of the Argon gas surrounding the fireball (0.05 eV, 0.1 eV, 0.5 eV, 0.7 eV, and 1.0 eV). Each of these represent an equilibrium temperature that would be reached for different mass flow rates of the Argon gas through the cavity. For the purposes of the discussion about the detail of the fireball dynamics, the 0.1 eV case will be used. The pressure profiles for the expanding fireball are shown in Fig. 1 for this representative case. From $t = 4.2 \times 10^{-3}$ ms until $t = 0.46$ ms, the shock front is broadened by radiant preheating of the gas. This is also shown in the gas temperature profiles in Fig. 2. By $t = 0.46$ ms, the plasma temperature has dropped below 1 eV and the fireball has become transparent to its own radiation. This is apparent from Fig. 3 which shows that the Planck and Rosseland mean free paths for argon at $N_p = 1.67 \times 10^{18}$ cm^{-3} increase dramatically once $T_r = T_p$ drops below ~ 1 eV. Thus, just as is well known for explosions in atmospheric air,[14] the gas becomes transparent once $T_r = T_p$ falls below the transparency temperature. In this case, the transparency temperature

Table 1

Input Parameters for FIRE Calculations

Cavity radius	4 meters
Gas type	Argon
Gas pressure at $0^{o}C$	50 torr
Gas number density	1.67×10^{18} cm^{-3}
Gas mass density	1.114×10^{-4} gm/cm^{3}
Energy deposited in fireball	30 MJ
Initial fireball radius	10 cm
Initial fireball temperature	64 eV
Initial fireball charge state	12

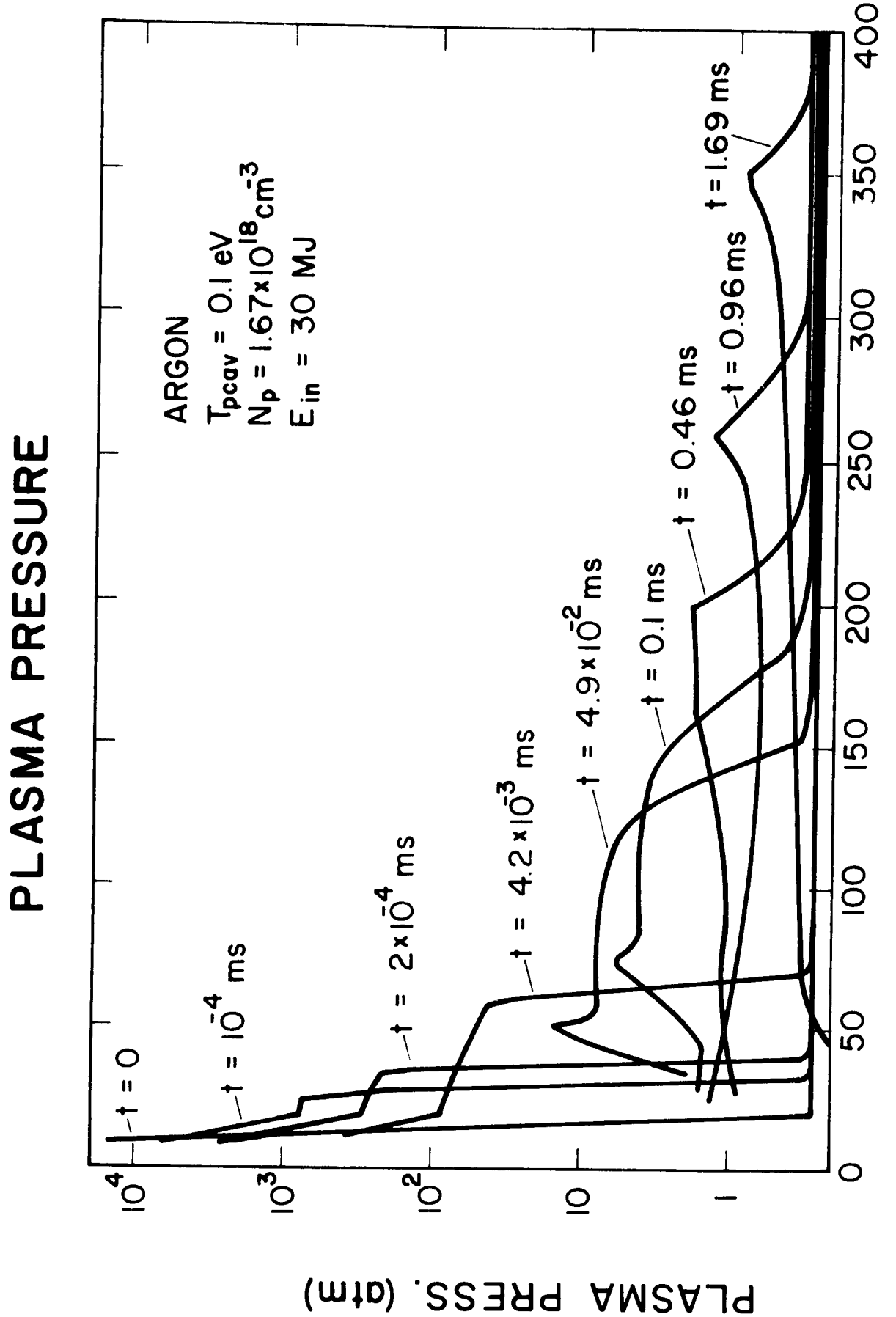

Figure 1 Gas pressure profiles at various times for a 30 MJ explosion in 1.67 x 10^{18} cm^{-3}, 0.1 eV Argon gas.

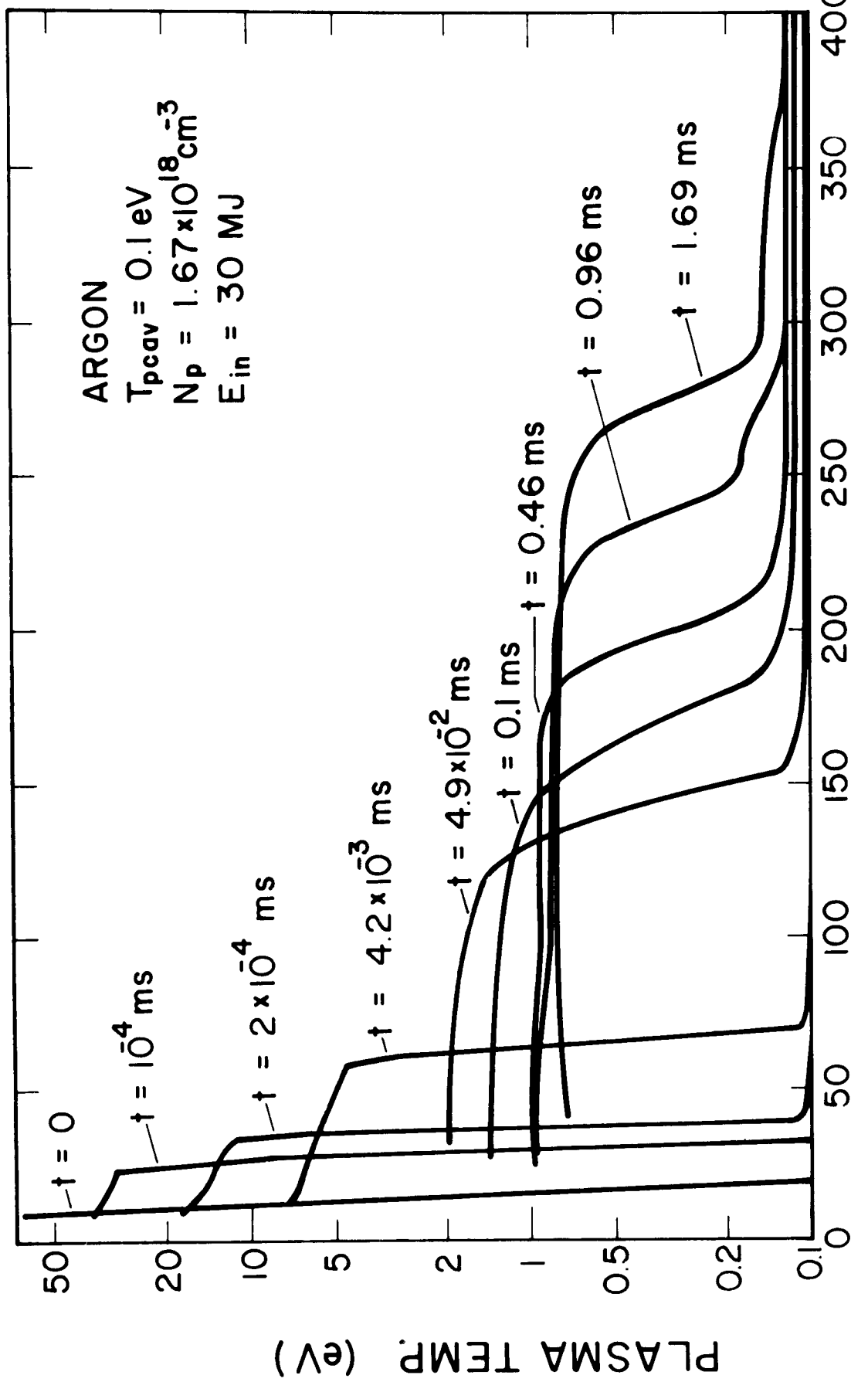

Figure 2 Gas temperature profiles at various times for a 30 MJ explosion in 1.67 x 10^{18} cm^{-3}, 0.1 eV Argon gas.

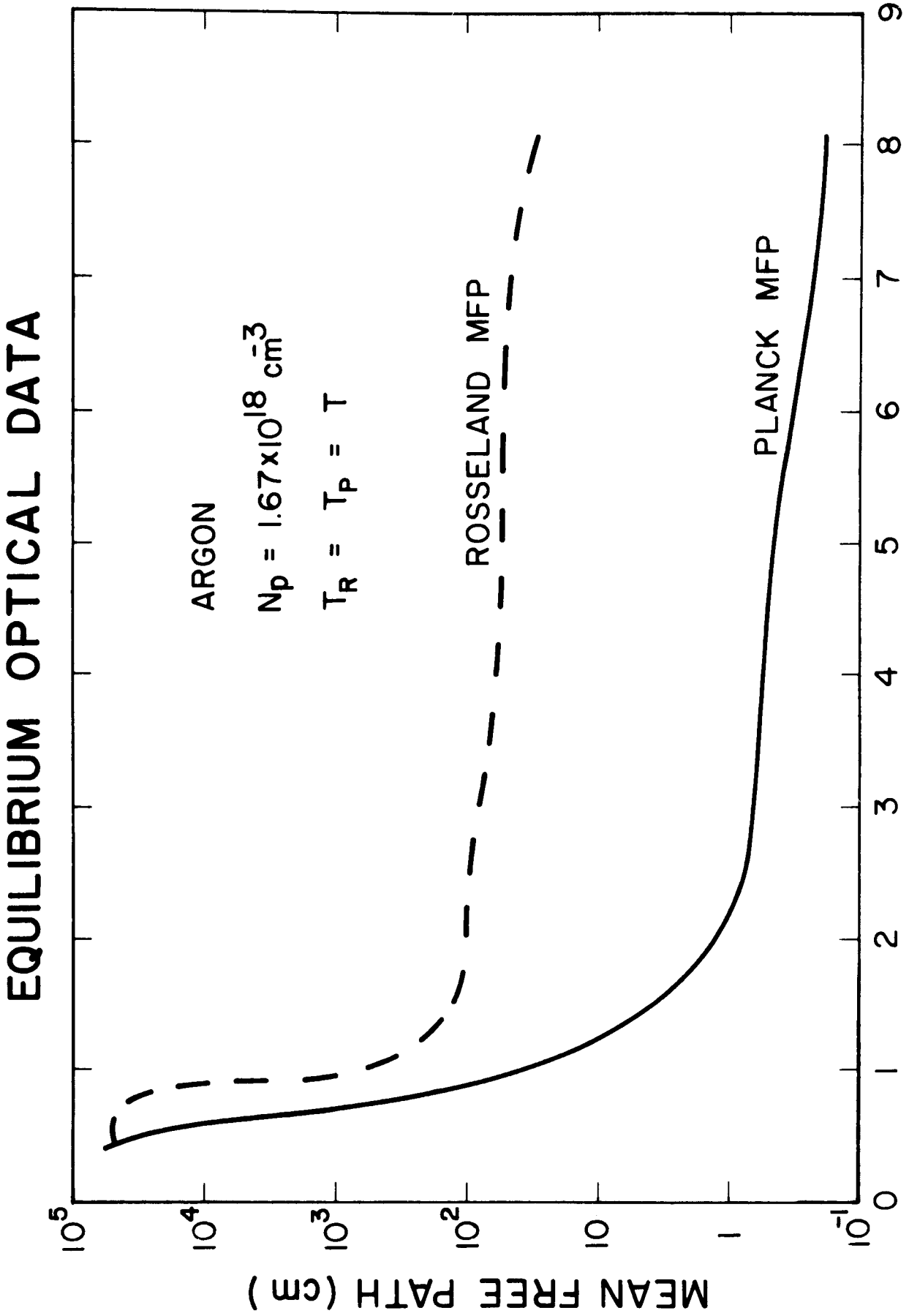

Figure 3 Rosseland and Planck mean free paths for radiation in 1.67×10^{18} cm^{-3} Argon. The radiation is assumed to be in equilibrium with the gas so that $T_r = T_p = T$.

is 1 eV, while air does not become transparent until T_p drops below 0.2 eV. At t = 1.69 ms, the shock front separates from the fireball, held behind 270 cm. This becomes evident from comparing the pressure and temperature profiles in Figs. 1 and 2. The maximum pressure occurs at a radius of 350 cm. Again, this phenomenon is well established from atmospheric fireball events.[14] The results of this calculation deviate significantly from the Taylor-Sedov theory discussed in Section III. This deviation becomes apparent in Fig. 4, where the positions of each of the 50 zones are plotted against time. Here, the position of the shock front as it would be for a 30 MJ strong shock is also plotted against time. This deviation occurs because the radiation mean free paths become large early in the calculation so that radiant energy leaks from the fireball, thus reducing the driving pressure and hence the blast slows its propagation. This characteristic of argon gas that allows radiation to leak from the fireball before the blast wave reaches the first wall has serious consequences for light ion beam fusion reactor designs. Such a result could be good because the strength of the blast wave is reduced, thus reducing the overpressure. On the other hand, the heat flux experienced by the first wall will be large and this will pose serious questions about its thermal response. The key to this problem is the rather high transparency temperature of argon (and other noble gases as well).

The overpressure and heat flux experienced by the first wall in the previous fireball calculation are shown in Fig. 5. As previously mentioned, the radiation mean free paths become long very early in the history of the explosion. Thus, during the first 0.5 ms after the start of the explosion, the fireball releases 6.4 MJ of radiant energy to the wall. The heat flux increases rapidly as a function of time because

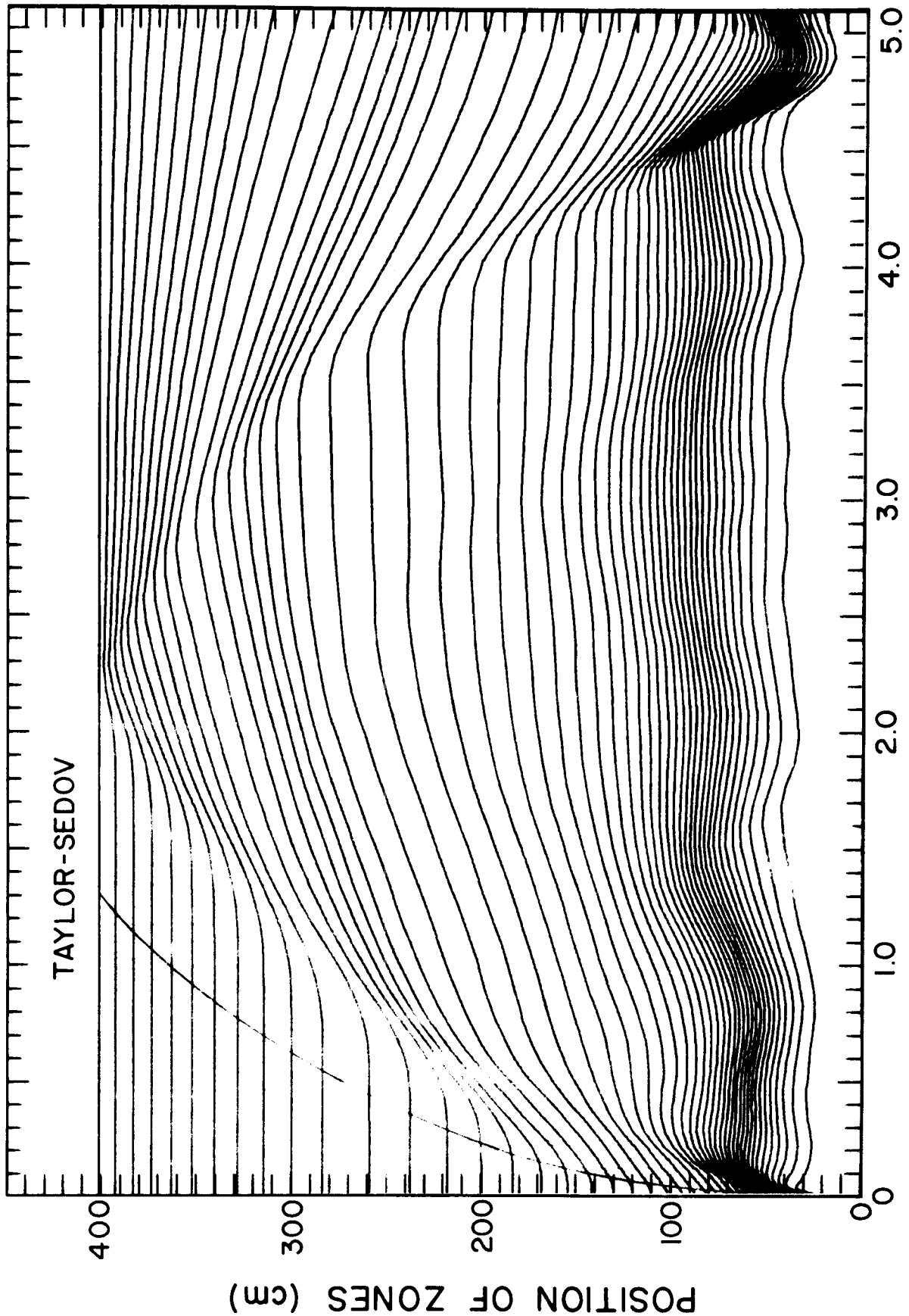

Figure 4 Propagation of a 30 MJ shock through a 1.67 x 10^{18} cm^{-3}, 0.1 eV Argon gas. The positions of the boundaries of 50 Lagrangian zones are plotted against time as is the position of shock front predicted by strong shock theory.

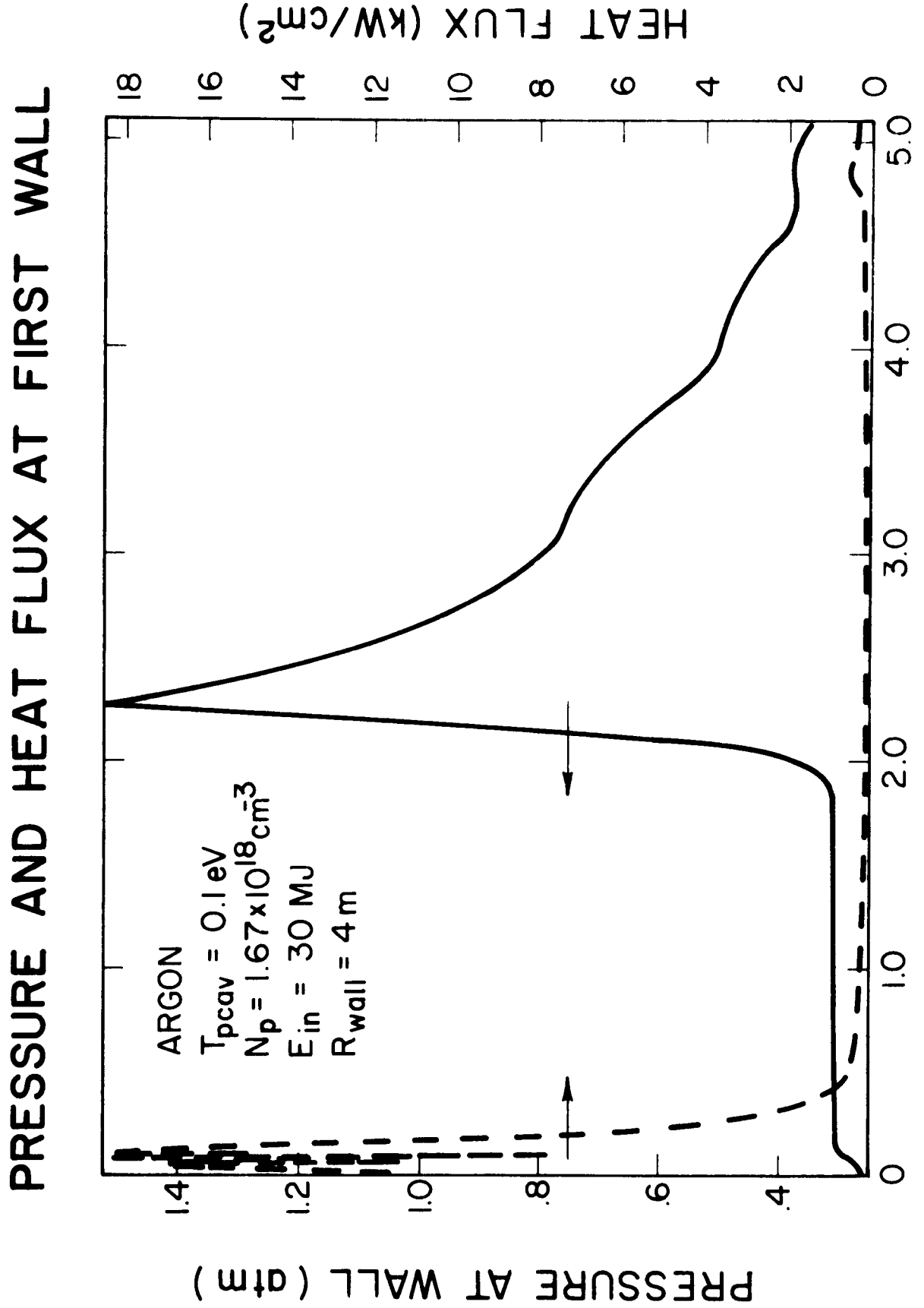

Figure 5 Pressure and heat flux at a 4 meter radius first wall. A 30 MJ shock propagates through 1.67 x 10^{18} cm^{-3}, 0.1 eV Argon gas.

the transparency transition in the gas is so abrupt. Since radiant energy is proportional to T_r^4, the resulting drop in fireball temperature after it becomes transparent reduces the radiant energy in the fireball to negligible values and the radiant heat flux to the wall ceases. The pressure on the wall remains low until the shock reaches it, as is easily seen by comparing Figs. 4 and 5. The maximum pressure is higher than would be expected from Fig. 1, because the pressure behind a reflected shock is higher than that behind the incident shock, which we showed in Section III.

By changing the cavity gas from an inert gas to a diatomic gas (such as N_2), the early release of radiant energy from the fireball might be avoided. This will occur because a diatomic gas has low lying molecular vibrational states not present in monatomic gases. Thus, low energy photons, which are only weakly absorbed in Argon, will be stopped more effectively in N_2. Such additional photon absorption mechanisms will decrease the transparency temperature. This effect has been estimated by using the optical data for Argon but requiring that the mean free paths are less than 50 cm for T_r less than 1.5 eV. This can be called "diatomic Argon". The wall pressure and heat flux are shown in Fig. 6 for the example case where the optical data have been altered in this way. This clearly shows that the radiant heat will now not prematurely leak from the fireball and the maximum heat flux will be reduced significantly (0.12 kW/cm^2 compared with 18 kW/cm^2). There are other changes in the behavior of the blast wave: the shock arrives at the first wall earlier because the fireball more closely meets the conditions of strong shock theory and the maximum wall pressure is higher because there is less energy lost through radiation and because the shock front is less broadened by radiative heat conduction.

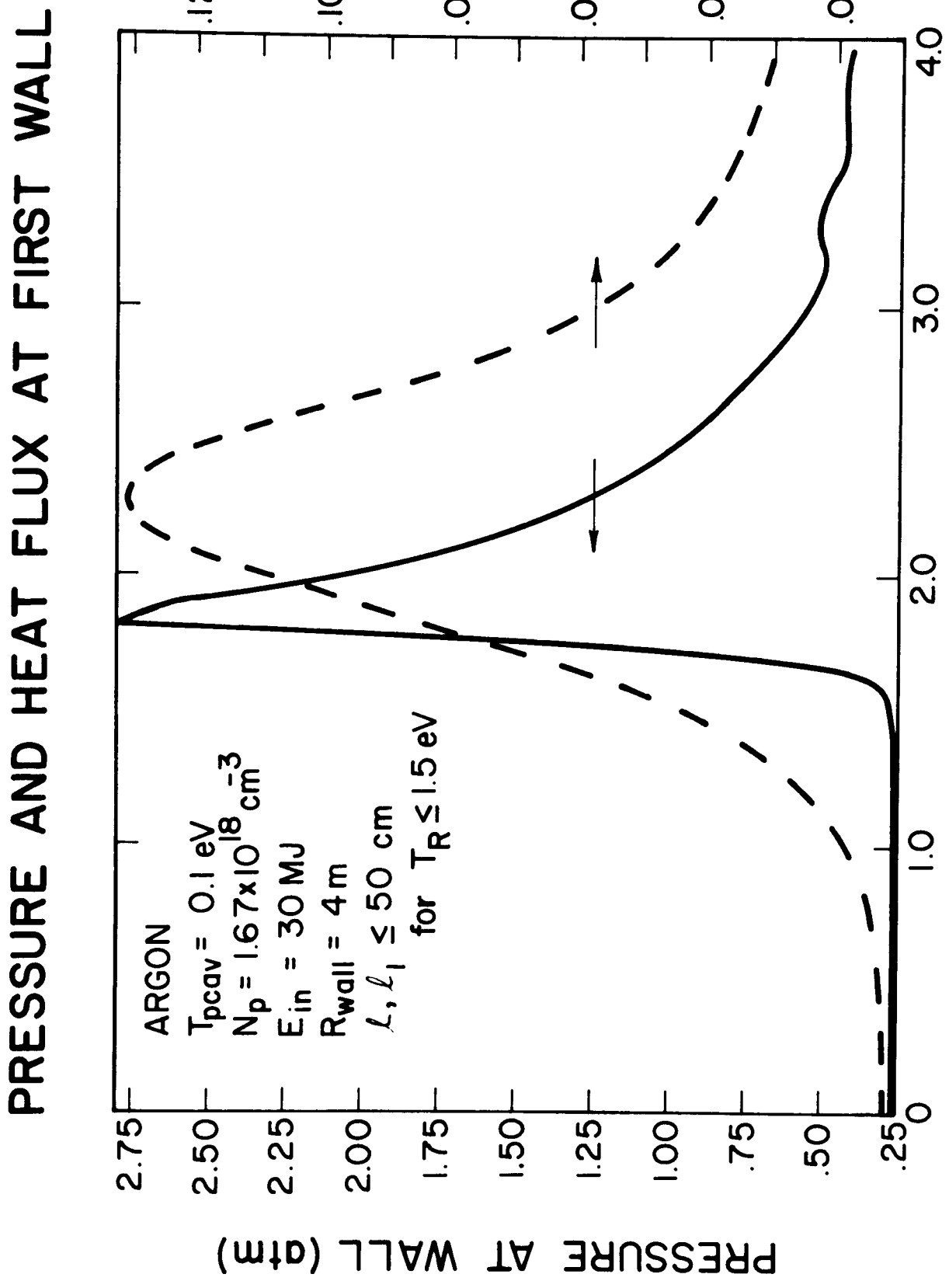

Figure 6 Pressure and heat flux at a 4 meter radius first wall. A 30 MJ shock propagates through 1.67 x 10^{18} cm^{-3}, 0.1 eV "diatomic Argon". The radiation mean free paths are those of Argon except when $T_r < 1.5$ eV, where they are no larger than 50 cm.

Similar calculations for Argon gas have been done at other initial gas temperatures. The results of these calculations are shown in Table 2. The maximum overpressure on the wall increases because the initial gas pressure is higher with increasing temperature. The total radiant energy transferred to the first wall also increases with energy. This is because the gas surrounding the fireball has an increasing amount of energy associated with it as its temperature increases. At a temperature of 1.0 eV for instance, there is more energy radiated to the wall (148 MJ) than is in the fireball. This is clearly a non-physical result. The point to be made here is that at a gas temperature between 0.7 eV and 1.0 eV (actually ~ 0.73 eV) the gas will radiate 30 MJ to the wall for every 30 MJ deposited into it. At this equilibrium point no gas circulation through the cavity is needed to maintain cyclic steady-state operation at this temperature. To maintain cyclic steady-state temperatures below 0.73 eV, the gas must be circulated through an external heat exchanger.

A gas with a large heat capacity might be expected to reduce the fluxes of radiant energy reaching the first wall. This will occur because the temperature of the gas would be lower for the same energy content so that the energy density associated with radiation coupled to this gas would be lower. With less radiant energy in the system, the radiation reaching the wall might be lower. This conjecture has been verified by carrying out a calculation for a 50 torr xenon gas, which has a higher heat capacity than Argon because it is more easily ionized. We have considered the case where a 4 meter cavity is filled with xenon at a temperature of 0.1 eV. As is shown in Fig. 7, the overpressure at the first wall is the same for

Table 2

Wall Overpressures and Radiant Heat Fluxes for Argon Cavity Gas at Different Temperatures

E_{in} = 30 MJ		$N_p = 1.67 \times 10^{18}$ cm^{-3}			R_{wall} = 4 m
T_p cav (eV)	$P_{wall-max}$ (atm)	$P_{initial}$ (atm)	ΔP (atm)	E_{out} (MJ)	$\langle q" \rangle_{pulse}$ (kW/cm^2)
0.05	1.3	.113	1.17	6.6	21.9
0.1	1.5	.275	1.23	7.5	15.0
0.5	2.5	1.33	1.17	14.7	24.5
0.7	2.75	1.98	.78	20.3	29.2
1.0	3.0	2.95	.05	148	52.6

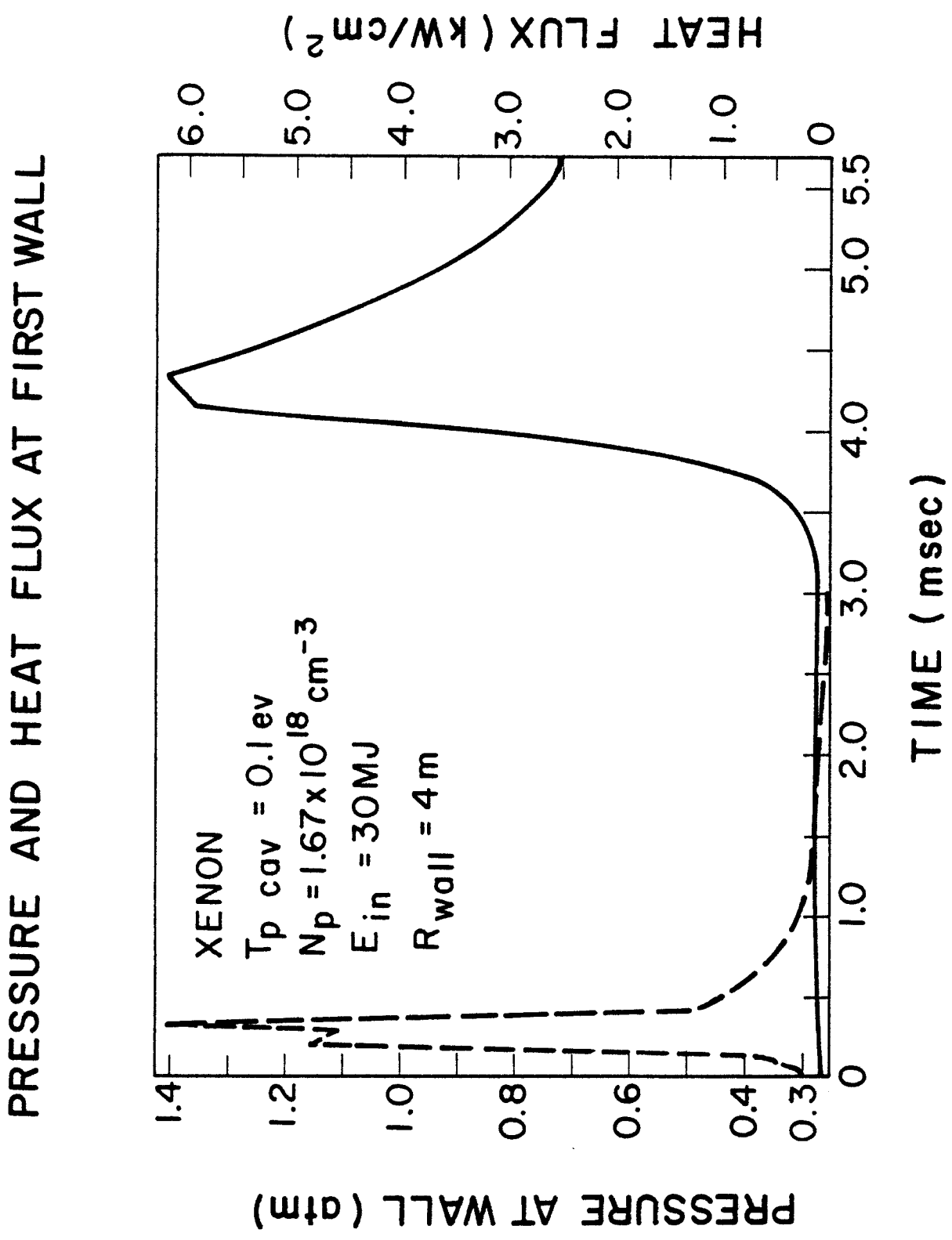

Figure 7 Pressure and heat flux at a 4 meter radius first wall. A 30 MJ shock propagates through 1.67 x 10^{18} cm^{-3}, 0.1 eV Xenon gas.

both Xenon and Argon while the pulse averaged heat flux for Xenon is reduced to 5 kW/cm^2. The total radiated energy per shot is 3.5 MJ, which may be compared with 7.5 MJ for Argon. Because there is less heat reaching the first wall with no increase in overpressure, it should be easier to design the walls of a Xenon gas filled cavity.

V. Conclusions

Shock propagation though Argon cavity gas for various gas temperatures has been computed using a hydrodynamic-radiative transport computer code especially designed for this purpose. From these calculations several general conclusions can be drawn.

(1) The strong shock theory of Taylor, et al.[2-4] does not adequately treat the propagation of a fireball through typical ion beam fusion reactor cavities.

(2) The gas temperature and gas pressure profiles indicate that a shock wave separates from the fireball long before it reaches the wall of a 4-meter radius cavity.

(3) Radiant heat fluxes measured at the first wall are large for Argon gas at a density of 1.67×10^{18} cm^{-3} and they increase with increasing cavity gas temperature.

(4) The maximum overpressure at the first wall increases with increasing cavity gas temperature.

(5) Diatomic gases may be better suited than noble gases for the cavity gas in light ion beam fusion reactors because indications are that they will not become transparent and volumetrically radiate their energy to the first wall once the gas temperature drops below 1 eV.

(6) On the other hand, if a large heat flux can be tolerated then noble gases offer the opportunity to reduce the overpressure created by the blast wave by radiating away much of the fireball energy.

(7) Because of its larger heat capacity, Xenon gas may be more effective than Argon in protecting the first wall from large radiant heat fluxes.

Acknowledgement

This research was supported by Sandia Laboratory, Albuquerque, NM, under contract to the United States Department of Energy.

REFERENCES

1. T.J. McCarville, private communication.

2. G. Taylor, Proc. R. Soc., A201, 159 (1950).

3. D.A. Freiwald and R.A. Axford, J. Appl. Phys., 46, 1171 (1975).

4. L.D. Landau and E.M. Lifshitz, Fluid Mechanics, Addison-Wesley, Reading, Massachusetts, 392-394 (1959).

5. Ya. B. Zel'dovich and Yu. P. Raizer, Physics of Shock Waves and High-Temperature Hydrodynamic Phenomena, Academic Press, New York, New York, 168-172 (1962).

6. R.D. Richtmyer and K.W. Morton, Difference Methods for Initial Value Problems, Wiley, New York, New York, 311-320 (1967).

7. Ibid., 17.

8. R. Courant and K.O. Friedrichs, Supersonic Flow and Shock Waves, Interscience Publishers, New York, New York, (1948).

9. L. Spitzer, Physics of Fully Ionized Gases, Interscience Publishers, New York, New York, (1962).

10. R.R. Peterson and G.A. Moses, MFP—A Calculation of Radiation Mean Free Paths, Ionization and Internal Energies in Nobel Gases, University of Wisconsin Report UWFDM-307 (1979).

11. Ya. B. Zel'dovich and Yu. P. Raizer, Physics of Shock Waves and High-Temperature Hydrodynamic Phenomena, Academic Press, New York, New York, Chapter III (1967).

12. L.D. Landau and E.M. Lifshitz, Fluid Mechanics, Addison-Wesley, Reading, Massachusetts, 329-331 (1959).

13. Ibid., 365.

14. Ya. B. Zel'dovich and Yu. P. Raizer, Physics of Shock Waves and High-Temperature Hydrodynamic Phenomena, Academic Press, New York, New York, 611-621 (1967).